SPE 7452

RESERVOIR LIMIT TESTING FOR FRACTURED WELLS

by Alain C. Gringarten, Flopetrol

This paper was presented at the 53rd Annual Fall Technical Conference and Exhibition of the Society of Petroleum Engineers of AIME, held in Houston, Texas, Oct. 1-3, 1978. The material is subject to correction by the author. Permission to copy is restricted to an abstract of not more than 300 words. Write: 6200 N. Central Expy., Dallas, Texas 75206.

ABSTRACT

The purpose of the paper is to extend reservoir limit test analysis techniques to fractured wells. By deriving the pseudo-steady state pressure functions for an unfractured and a fractured well at any position of a closed rectangle, it is shown that shape factors for fractured wells are not readily obtainable from the ones for unfractured wells.

Exact analytical expressions of shape factors for fractured and unfractured wells in a closed rectangle are presented, along with graphs of these quantities versus appropriate parameters.

Type curves for a fractured well at the center of a closed rectangle are also provided. Both uniform flux and infinite conductivity fractures are considered.

The curves presented in this paper are then used with actual field data for estimating the drainage volume of a fractured well and the shape of the well drainage area.

INTRODUCTION

Reservoir limit tests, introduced by Jones[1], are commonly used for evaluating the reservoir volume communicating with the well. The analysis is based on the fact that the well pressure during pseudo-steady state flow is a linear function of the production time :

$$p_{wf} = m^* t + p_{int} \tag{1}$$

where

$$m^* = \frac{0.234\ qB}{\phi c_t\ hA} \tag{2}$$

and

$$p_{int} = p_i - \frac{70.60\ qB\mu}{kh}\left[\ln\left(\frac{A}{r_W{}^2}\right) + \ln\left(\frac{2.246}{C_A}\right) + 2S\right] \tag{3}$$

A represents the drainage area (in sq.ft) and C_A the drainage area shape factor. Eq.1 may also be written in dimensionless form as :

$$p_D = 2\pi t_{DA} - \ln\frac{rw}{\sqrt{A}} - \frac{1}{2}\ln C_A + 0.4045 + S \tag{4}$$

with

$$p_D = \frac{kh\ (p_i - p_{wf})}{141.2\ qB\mu} \tag{5}$$

and

$$t_{DA} = \frac{0.000264\ t}{\phi\mu C_t\ A} \tag{6}$$

A cartesian plot of bottom-hole flowing pressure versus production time will thus yield a straight line after pseudo-steady state conditions are reached. The slope of the straight line (Eq.2) may be used to estimate the connected reservoir drainage volume :

$$\phi hA = -\frac{0.234\ q_B}{C_t\ m^*} \tag{7}$$

and the drainage area, if ϕh is known.

The shape of the drainage area may be estimated from the pseudo-steady state cartesian plot if pressure data are also available from an infinite acting flow period[2]. These are used to determine the semi-log straight line slope :

$$m = \frac{162.6\ qB\mu}{kh} \tag{8}$$

and p_{1hr}. The system shape factor is then obtained from :

$$C_A = 5.456\frac{m}{m^*}\exp\left[2.303\ \frac{p_{1hr} - p_{int}}{m}\right] \tag{9}$$

By comparing the calculated C_A with the ones published in the literature for various drainage area configuration[3-5], it is possible to estimate the shape of the drainage area.

As an additional (although insensitive) check it was suggested[2] to also compute the dimensionless

References and illustrations at end of paper.

time corresponding to the beginning of pseudo-steady state behavior :

$$(t_{DA})_{pss} = 0.1833 \frac{m^*}{m} t_{pss} \qquad (10)$$

(where t_{pss} is the time at start of the actual pseudo-steady state straight line), and to compare it with the tabulated theoretical values.

The analysis method presented above is applicable to gas reservoirs and injection testing as well as to liquid reservoirs and drawdown testing. It does not apply to wells intersecting fractures. The purpose of the present paper is to extend these reservoir limit test analysis techniques to fractured wells.

SHAPE FACTORS FOR UNFRACTURED WELLS

The shape factor C_A that appears in Eq.3, was first introduced by Brons and Miller[6] for relating the pseudo-steady state flowing pressure p_{wf} to the average static pressure $\bar{p}$ in the area drained by the well. In Darcy units, this is expressed as :

$$\bar{p} - p_{wf} = \frac{q\mu}{4\pi kh} \ln \frac{A}{\gamma C_A r'^2_w} \qquad (11)$$

Eq. 11 is valid for any drainage area configuration. It is identical to Eq.4, as $\bar{p} = 2\pi t_{DA}$; γ is the exponential of Euler's constant and is equal to 1.781.r'_w is the effective wellbore radius, which includes any positive or negative skin factor ($r'_w = r_w e^{-s}$).

Values of the shape factor C_A were obtained by Brons and Miller[6] from pseudo-steady state pressure versus time curves published by Matthews, Brons and Hazebroek[7] for various drainage area shapes. This work was further extended by Dietz[3], and Earlougher, et al.[8] Dietz also provided limits of validity of the pseudo-steady state flow equation, Eq.11.

Additional information on shape factors for rectangular reservoirs was presented by Earlougher and Ramey[9], who provided plots of C_A against various shape-determining quantity, such as well location or length-to-width ratio. The plots were constructed from C_A values tabulated by Brons and Miller[6], and Dietz[3], or obtained by using superposition techniques described by Ramey[10] and Earlougher, et al.[9] Earlougher and Ramey[9] noticed that the shape factor was becoming very small as the well approached a drainage boundary. They suggested that, in such a case, the shape factor was no longer constant, but could be proportional to some power of (r_w^2/A).

We present in Appendix A an exact analytical expression for the shape factor in the case of a well at any position in a closed rectangle (Fig.1).

Details of the derivation are given in Appendix A. It is shown that C_A depends upon the length-to-width ratio x_e/y_e, the well location (x_w/x_e, y_w/y_e) and $r_w/\sqrt{A}$. C_A is independant of $r_w/\sqrt{A}$ only at very low values of this parameter.

As an example, ln C_A was calculated for a well at the center of a closed rectangle. The result is shown on Fig.2, as a function of $r_w/\sqrt{A}$, for various x_e/y_e values. Fig.2 clearly indicates the variation of C_A with $r_w/\sqrt{A}$. Only when $r_w/\sqrt{A} < 10^{-6}$ are the C_A's calculated in the present paper identical to those available in the literature[3-5].

FRACTURED WELL IN A CLOSED RECTANGLE

Type curves for a well with a uniform flux or an infinite conductivity vertical fracture at the center of a closed square were published by Gringarten et al.[11]. These curves indicates that vertically fractured systems exhibit a pseudo-steady state behavior similar to that of unfractured ones. The general pseudo-steady depletion equation presented by Brons and Miller (Eq.4 or 11) was used by Gringarten, et al.[12] to calculate an effective well radius, with a C_A equal to that of an unfractured well at the center of a closed square.

The effective wellbore radius was found to depend upon the nature of the fracture (uniform flux versus infinite conductivity), and to vary with the fracture penetration ratio, x_f/x_e.

Earlougher[5] suggested to use Eq.4 for representing the pseudo-steady state behavior of a vertically fractured well at the center of a closed square, with x_f/x_e substituted for $r_w/\sqrt{A}$ and provided a list of C_A values for various fracture penetration ratios, x_f/x_e. These C_A values, however, are only valid for infinite conductivity fractures, and appear to have been derived from the vertical fracture pressure versus time dimensionless data published by Russell and Truitt. These data were in good agreement with those later published by Gringarten, et al.[11], except for $x_f/x_e = 0.1$, in which case Russell and Truitt's[13] results are believed to be erroneous. It is therefore likely that Earlougher's C_A value for $x_f/x_e = 0.1$ is not correct. Except for this restriction, it is actually equivalent to use Eq.4 with an effective wellbore radius depending upon x_f/x_e and the C_A value for an unfractured well at the center of a closed square, or to substitute x_e/x_f for $\sqrt{A}/r_w$ into Eq.4 and to use a C_A depending upon x_f/x_e.

In order to further compare the pseudo-steady state behavior of unfractured, and fractured wells, type-curves were computed for a well with a vertical fracture in a closed rectangle (Fig.3). For this purpose, the dimensionless pressure drop function presented by Gringarten et al. (Eq.27 of Ref.12) was modified in order to include characteristic dimensionless parameters. The result is given in Appendix B.

The dimensionless pressure p_D for a vertically fractured well in a closed rectangle is thus a function of t_{DA}, $x_f/\sqrt{A}$, the length-to-width ratio x_e/y_e, the position of the well in the rectangle (x_w/x_e, y_w/y_e) and the location of the pressure point relative to the fracture (x/x_f, y/x_f. xf is the fracture half length.

As indicated in Ref.12, the well pressure for a uniform flux fracture is obtained with $x/x_f = y/x_f = 0$, whereas that for an infinite conductivity fracture corresponds to $x/x_f = 0.732$ and $y/x_f = 0$.

TYPE - CURVES

Type-curves for a well at the center of a closed rectangle, with a uniform flux, or an infinite conductivity vertical fracture, are shown on Figs. 4 and 5, respectively for various values of $x_f/\sqrt{A}$ (0.5, 0.3, 0.2, 0.15, 0.10, 0.05 and 0), and of x_e/y_e (1/4, 1/2, 1, 2, and 4). As in Ref.11, the x axis is labelled in terms of :

$$t_{Df} = \frac{k\ t}{\phi\mu C_t\ x_f^2} = t_{DA} \Big/ \left(\frac{x_f}{\sqrt{A}}\right)^2 \qquad (12)$$

The shape of these type curves is similar to that for a vertically fractured well at the center of a closed square[11], which were given as a function of the reciprocal of the fracture penetration ratio x_e/x_f. Some of the curves are actually identical. The correspondance beetween x_e/x_f and $x_f/\sqrt{A}$ is provided in Table 1 for the various x_e/y_e values.

One important feature on Figs.4 and 5 is the fact that all the curves corresponding to a specific $x_f/\sqrt{A}$ value become identical at long times, when pseudo-steady state conditions are reached, for all x_e/y_e values. They differ only during the late transient flow period. Because of the relative position of the curves, however, it would be difficult to estimate the correct length to width ratio from a type curve match. For instance, if only transient and late transient data were available, it would not be possible to differentiate between $x_f/\sqrt{A} = 0.15$ and $x_e/y_e = 4$ or 1/4; and $x_f/\sqrt{A} = 0.20$ and $x_e/y_e = 1.2$ or 1/2. In any case, it is not possible to distinguish between $x_e/y_e = 2$ and $x_e/y_e = 1/2$, or between $x_e/y_e = 4$ or $x_e/y_e = 1/4$, if $x_f/\sqrt{A}$ is less than 0.20.

As a consequence, erroneous distances to boundaries are likely to be obtained if the wrong set of dimensionless parameters is selected. This would be particularly true if the closed square vertical type curves of Ref.11 are used for interpreting data from a well in a closed rectangle. On the other hand, k_h and x_f deducted from the match should be correct.

SHAPE FACTOR

A pseudo-steady state flow function for a vertically fractured well in a closed rectangle, is derived in Appendix B. The result can be written as :

$$p_D = 2\pi t_{DA} + (p_{int})_{Df} \qquad (13)$$

where $(p_{int})_{Df}$ is the intercept (dimensionless) of the pseudo-steady state cartesian straight line $(p_{int})_{Df}$ is given as an exact analytical expression involving the drainage area length to width ratio x_e/y_e, the position of the well in the rectangle $(x_w/x_e,\ y_w/y_e)$, and the location of the pressure point relative to the fracture $(x/x_f,\ y/x_f)$.

Fig.6 and 7 show semi-log plots of $(p_{int})_{Df}$ versus $x_f/\sqrt{A}$, for a uniform flux and an infinite conductivity vertical fracture, respectively. We notice that, at low $x_f/\sqrt{A}$ values (less than 0.05), the various curves become parallel straight lines and it is not possible to differentiate between a particular x_e/y_e value and its reciprocal. This is in line with what was observed on the type curves•.

The slope of the low $x_f/\sqrt{A}$ value straight lines on Fig.6 and 7 is equal to 2.303, which suggests that $(P_{int})_{Df}$ is a linear function of $\ln(x_f/\sqrt{A})$. Thus, by defining the shape factor C_f for a vertically fractured well as :

$$p_D = 2\pi t_{DA} - \ln\frac{x_f}{\sqrt{A}} - 1/2\ln C_f + 0.4045 \qquad (14)$$

one obtains the shape factor curves shown in Figs.8 and 9.

Eq. 14 is similar to Eq.4 or Eq.11, with x_f substituted for r_w and C_f for C_A. By comparing Fig.2 with Figs.8 and 9, it is found that at low $x_f/\sqrt{A}$ values (less than 0.05), and for any x_e/y_e value :

$$1/2\ln C_A = 1/2\ln C_f + 1, \text{ for a uniform flux fracture} \qquad (15)$$

$$1/2\ln C_A = 1/2\ln C_f + 0.6932 \text{ for an infinite conductivity fracture} \qquad (16)$$

This checks with the transient flow functions derived by Gringarten, et al.[12], which read :

$$p_D = 1/2\,(\ln t_{Df} + 0.80907) + 1, \text{ for a uniform flux fracture} \qquad (17)$$

and

$$P_D = 1/2\,(\ln t_{Df} + 0.80907) + 0.6932, \text{ for an infinite conductivity fracture} \qquad (18).$$

In other words, for $x_f/\sqrt{A}$ less than 0.05, the pseudo-steady state behavior of a vertically fractured well at any x_e/y_e value can be represented by Eq.4 or 11, with a shape factor equal to that of an unfractured well, with the same x_e/y_e value (or its reciprocal), and an effective wellbore radius equal to :

$$r'_w = x_f/2.718, \text{ for a uniform flux fracture} \qquad (19)$$

$$r'w = x_f/2\quad, \text{ for an infinite conductivity fracture} \qquad (20)$$

This could be also used for $x_f/\sqrt{A}$ values higher than 0.05, but the effective wellbore radius would then vary with $x_f/\sqrt{A}$ and x_e/y_e, which makes this approach impractical. Eq.14 should be used in that case, with C_f from either Fig.8 or Fig.9.

PSEUDO-STEADY STATE FLOW DATA INTERPRETATION

The material presented above can be used to analyze reservoir limit tests. The procedure is as follows :

1. plot both $\Delta p = p_i - p_{wf}$ or $\Delta p = p_{wf}\ (t = 0) - p_{wf}$ vs t on log-log paper; and p_{wf} vs t on cartesian paper.

2. from the shape of the log-log curve, determine whether the well is fractured or not. If the well is fractured (the early time data fall on a log-log straight line of slope 0.5), find the best match on either Fig.4 or Fig.5 . Calculate $\frac{kh}{141.2\ qB\mu}$ and kh from the pressure match, and x_f from the time match. $kh/141.2\ qB\mu$ is simply equal to the ratio of the dimensionless pressure to the real pressure at the match point.
If semi-log analysis is applicable, that quantity is also given by $1.151/m$.

3. from the pseudo-steady state cartesian plot, find m* and p_{int}.

• Large scale copies of Figs. 4 to 7 are available from the author on request.

4. calculate the drainage area : $A = \frac{-0.234\,qB}{\phi h c_t\, m^*}$

5. calculate $x_f/\sqrt{A}$ and $(P_{int})_{Df}$ =

$$\frac{kh}{141.2qB\mu}\,(P_i - P_{int})$$

6. read x_e/y_e from the appropriate Fig.6 or 7 (depending on the type-curve that provides the best match in 3).

7. check that the calculated $x_f/\sqrt{A}$ and the resulting x_e/y_e are in good agreement with the type-curve match.

It should be noted that the determination of the drainage area length-to-width ratio alone depends only on the property of the data plots, and do not require knowledge of reservoir properties nor production characteristics (except for p_i or p_{wf} at $t = 0$). Fig. 6 or Fig.7 coordinates are simply obtained as :

$$x_f/\sqrt{A} = 24.6\sqrt{-\,m^*\left(\frac{p_D}{\Delta p}\right)^* \left(\frac{t}{t_D}\right)^*} \qquad (21)$$

and

$$(p_{int})_{Df} = \left(\frac{p_D}{\Delta p}\right)^* (p_i - p_{int}) \qquad (22)$$

where the symbol * refers to the match point.

EXAMPLE CALCULATION

To illustrate the technique outlined above, we use pressure data from a 50 hour drawdown test in a Denver basin reservoir that were presented in Appendix D of Ref.4. The various test and reservoir characteristics are listed in Table 2.

1. a log-log plot of the data is shown in Fig.10, whereas Fig.11 presents a cartesian plot of the same data.

2. early time data on Fig.10 fall on a log-log straight line of slope 0.5, which suggests that the well is fractured. The best match is achieved with the type curves for an infinite conductivity fracture (Fig.5) and is shown on Fig.12. From the pressure match ($p_D = 0.28$; $\Delta p = 100$psi) one obtains :

$$k = \frac{141.2\,qB\mu}{h}\left(\frac{p_D}{\Delta p}\right)^* = \frac{141.2 \times 800 \times 1.25 \times 1.0 \times 0.28}{8 \times 100} = 49\text{md}$$

whereas the time match ($t_D = 0.023$, $t = 10$ mn) yields :

$$x_f = \left(\frac{0.000264\,k}{\phi \mu c_t}\,\frac{t}{t_D}\right)^{1/2} =$$

$$\left(\frac{0.000264 \times 49}{0.14 \times 1.0 \times 17.7\ 10^{-6}}\quad \frac{10}{0.023 \times 60}\right)^{1/2} = 194 \text{ ft}$$

3. from Fig.11 : $m^* = -15.8$ psi/hr and

$$p_{int} = 1520 \text{ psi}$$

4. $A = \frac{-0.234\,qB}{\phi h c_t\, m^*} = \frac{0.234 \times 800 \times 1.25}{0.14 \times 8 \times 17.7\ 10^{-6} \times 15.8} = 7.46\ 10^5$ sq.ft

5. $x_f/\sqrt{A} = \frac{194}{(7.46\ 10^5)^{1/2}} = 0.225$;

$$(p_{int})_{Df} = \frac{0.28}{100}(1895 - 1520) = 1.05$$

6. from Fig.13, we read $x_e/y_e = 2$ ($x_e/y_e = 0.8$ is also a possible result).

7. $x_f/\sqrt{A}$ from 5 and x_e/y_e from 6 agree well with the type curve match of Fig.12.

The above interpretation calls for a few comments. The permeability value ($k = 49$ md) obtained in step 2 agrees well with the result of the late transient analysis presented in Ref.4 ($k = 46$ md). Semi-log transient analysis was also used in Ref.4 but gave a much higher permeability ($k = 95$ nd). This anomaly was attributed to the fact that the well had been hydraulically fractured upon completion thus creating non radial flow distributions at early times. This is indeed true, as can be inferred from the type curve match of Fig.12 : the last pressure data point on the ($x_f/\sqrt{A} = 0$) curve (infinite acting fracture flow) corresponds to a dimensionless time equal to 1, whereas semi-log methods do not apply before $t_D = 4$.

The same example from Ref.4 was used by Earlougher in his publication on the use of reservoir limit tests for estimating drainage shapes[2]. As summarized at the beginning of the present paper (Eqs.7 to 10), Earlougher's work only concerned unfractured wells. The drainage area shape was estimated from a C_A value of 10.9, obtained by substituting into Eq.4, the same semi-log straight line slope value as in Ref.4 ($m = 212$ psi/cycle corresponding to $k = 95$ md). With Earlougher's values for m^*, p_{1hr} and p_{int}, Eq.4 read :

$$C_A = 5.456\,\frac{(-212)}{(-15.8)}\,\exp\left[2.303\,\frac{1.690 - 1.515}{-212}\right] = 10.9$$

Taking now the correct m value corresponding to $k = 49$ md ($m = 425$ psi/cycle) yields :

$$C_A = 5.456\,\frac{(-425)}{(-15.8)}\,\exp\left[2.303\,\frac{1.690 - 1.515}{-425}\right] = 56.9$$

This last C_A value does not correspond to any known drainage shape. In fact, it appears that the maximum possible C_A value is that for a well at the center of a closed circle ($C_A = 31.62$). Calculated C_A values higher than 31.62 are most likely erroneous. In our particular example, it proves that the reservoir limit test analysis techniques presented in Ref.2 for unfractured wells cannot be applied to fractured wells.

CONCLUSIONS

A simple technique was presented for estimating fractured well drainage area shapes from conventional reservoir limit tests. The method only requires knowledge of pressure data during pseudo-steady state and infinite acting flow periods. Evaluating the drainage area shape of a fractured well with methods designed for unfractured wells may lead to strongly erroneous results.

ACKNOWLEDGEMENTS

The author is grateful to the management of FLOPETROL for permission to publish this paper.

NOMENCLATURE

A	=	drainage area, sq.ft
B	=	formation volume factor, RB/STB
c_t	=	system total compressibility, psi^{-1}
C_A	=	shape factor for unfractured wells
C_f	=	shape factor for fractured wells
h	=	formation thickness, ft
k	=	permeability, md
m	=	$\pm$ slope of linear portion of semilog plot of pressure transient data, psi/cycle
m^*	=	slope of the straight line on a linear plot of p_w VS t, psi/hour
p	=	pressure psi
p_D	=	dimensionless pressure
p_i	=	initial reservoir pressure, or stabilized pressure at start of test, psi
p_{int}	=	pressure at intercept (abscissa value = 0)of the straight line on a cartesian plot of p_w vst, psi
$(p_{int})_{Df}$	=	pressure at intercept of the straight line on a cartesian plot of p_D vs t_{DA} for a fractured well
p_{1hr}	=	pressure on straight-line portion of semilog plot 1 hour after beginning a transient test
p_{wf}	=	flowing bottom-hole pressure, psi
Δp	=	pressure change, psi
q	=	flow rate, STB/D
r_w	=	wellbore radius, ft
r_w'	=	apparent or effective wellbore radius (includes effects of wellbore damage or improvement),ft
S	=	van Everdingen-Hurst skin factor
t	=	time, hours
t_D	=	dimensionless time based on half-fracture length of a vertical fracture
t_{DA}	=	dimensionless time based on drainage area
$(t_{DA})_{pss}$	=	dimensionless time at the beginning of pseudo-steady state flow
t_{pss}	=	time at the beginning of pseudo-steady state flow, hours
x	=	x coordinate, ft
x_e	=	x distance from the center to the edge of a rectangular drainage region (half-length of the side of a rectangle), ft
x_f	=	x distance from a well to the end of a vertical fracture centered at the well that is parallel to the x axis (half-length of a vertical fracture), ft
x_w	=	x distance from the center of a rectangular drainage region to the well, ft
y	=	y coordinate, ft
y_e	=	y distance from the center to the edge of a rectangular drainage region (half-length of the side of a rectangle), ft
y_w	=	y distance from the center of a rectangular drainage region to the well, ft
γ	=	exponential of Euler's constant = 1.781
μ	=	viscosity, cp
ϕ	=	porosity, fraction

REFERENCES

1. Jones, P : "Reservoir Limit Tests", Oil and Gas J (June 18, 1956) 54, N°59,184.
2. Earlaugher, R.C. Jr : "Estimating Drainage Shapes from Reservoir Limit Tests" J.Pet.Tech. (Oct 1971) 1266 - 1268, Trans AIME, 251.
3. Dietz, D.N. : "Determination of Average Reservoir Pressure from Build-up Surveys", J.Pet.Tech. (Aug 1965) 955 - 959.
4. Matthews C.S. and Russell, D.G. : "Pressure Build-up and Flow Tests in Wells", Monograph Series n°1, Society of Petroleum Engineers of AIME Dallas (1967).
5. Earlougher, R.C. Jr.: "Advances in Well Test Analysis", Monograph Series n°5, Society of Petroleum Engineers of AIME, Dallas (1977).
6. Brons F., and Miller, W.C. : "A simple Method for correcting Spot Pressure Readings", J. Pet. Tech. (Aug., 1961) 803 - 805.
7. Matthews, C.S., Brons, F. and Hazebroek, P. : "A Method for Determination of Average Pressure in a Bounded Reservoir", Trans. AIME (1954) 201, 182.
8. Earlougher, R.C., Jr., Ramey, H.J., Jr., Miller F.G. and Mueller, T.D. : "Pressure Distribution in Rectangular Reservoirs", J. Pet. Tech. (Feb., 1968) 199 - 208.
9. Earlougher, R.C., Jr. and Ramey, H.J., Jr. "The Use of Interpolation to Obtain Shape Factors for Pressure Build-up Calculations", J. Pet. Tech. (May, 1968) 449.
10. Gringarten, A.C., Ramey, H.J., Jr. and Raghavan, R. : "Applied Pressure Analysis for Fractured Wells", J. Pet. Tech. (July 1975) 887 - 892; Trans. AIME, 259.
11. Gringarten, A.C., Ramey,H.J., Jr. and Raghavan,R.: "Unsteady-State Pressure Distributions created by a Well With a Single Infinite-Conductivity Vertical Fracture", Soc. Pet. Eng. J. (Aug.,1974) 347 - 360.
12. Russell, D.G. and Truitt, N.E. : "Transient Pressure Behavior in Vertically Fractured Reservoirs", J. Pet. Tech. (Oct. 1964) 1159 - 1170; Trans. AIME 231.
13. Gringarten, A.C., and Ramey, H.J., Jr. : "The Use of Source and Green's Functions in Solving Unsteady Flow Problems in Reservoirs", Soc. Pet. Eng. J. (Oct. 1973) 285 - 296.
14. Gradshteyn, I.S., and Ryzhik, I.M. : "Tables of Integrals, Series and Products, Academic Press, New-York, London, 4th Ed. (1965).

APPENDIX A

SHAPE FACTOR FOR AN UNFRACTURED WELL IN A CLOSED RECTANGLE

A dimensionless pressure function for a well at any position in a closed rectangle has been obtained by Gringarten and Ramey in Ref.14 by means of source and Green's functions. With the well-reservoir system sketched in Fig.1, Eq.35 of Ref.14 becomes :

$$p_D = 2\pi t_{DA}$$

$$+ \frac{1}{\pi} \frac{x_e}{y_e} \sum_{n=1}^{\infty} \frac{1}{n^2} \left[1 - \exp\left(-n^2\pi^2 \frac{y_e}{x_e} t_{DA}\right)\right] \cos n\pi \frac{x_w}{x_e} \cos n\pi \left(\frac{x_w}{x_e} + \frac{x}{x_e}\right)$$

$$+ \frac{1}{\pi} \frac{y_e}{x_e} \sum_{n=1}^{\infty} \frac{1}{n^2} \left[1 - \exp\left(-n^2\pi^2 \frac{x_e}{y_e} t_{DA}\right)\right] \cos n\pi \frac{y_w}{y_e} \cos n\pi \left(\frac{y_w}{y_e} + \frac{y}{y_e}\right)$$

$$+ \frac{2}{\pi} \frac{x_e}{y_e} \sum_{m=1}^{\infty} \cos m\pi \frac{y_w}{y_e} \cos m\pi \left(\frac{y_w}{y_e} + \frac{y}{y_e}\right) \sum_{n=1}^{\infty} \frac{1 - \exp\left[-\left(n^2\frac{y_e}{x_e} + m^2\frac{x_e}{y_e}\right)\pi^2 t_{DA}\right]}{n^2 + \left(m\frac{x_e}{y_e}\right)^2} \cos n\pi \frac{x_w}{x_e} \cos n\pi \left(\frac{x_w}{x_e} + \frac{x}{x_e}\right) \quad \text{(A-1)}$$

Pseudo-steady state is reached when the exponential terms becomes negligible. This depends clearly on $\frac{y_e}{x_e}$, $\frac{x_e}{y_e}$ but also on the location of the well in the rectangle (x_w, y_w), and on that of the pressure point (x, y).
Considering the pseudo-steady state form of Eq. A-1, it is possible to find closed analytical expressions for the various summations, by using the following formulas [15]:

$$\sum_{n=1}^{\infty} \frac{\cos n\pi x}{n} = \frac{1}{2} \ln \frac{1}{2(1 - \cos \pi x)} = \frac{1}{2} \ln \frac{1}{4 \sin^2 \pi \frac{x}{2}} = - \ln 2 \sin \frac{\pi}{2} x \qquad 0 < x < 2$$

$$\sum_{n=1}^{\infty} \frac{1}{n^2} \cos n\pi x = \frac{\pi^2}{12} (2 - 6x + 3x^2) \qquad 0 \leq x \leq 2$$

$$\sum_{k=1}^{\infty} \frac{\cos k\pi x}{k^2 + \alpha^2} = \frac{\pi}{2\alpha} \frac{ch\alpha\pi (1-x)}{sh\alpha\pi} - \frac{1}{2\alpha^2} \qquad 0 < x < 2$$

$$\sum_{k=1}^{\infty} \frac{p^k \cos k\pi x}{k} = -\frac{1}{2} \ln (1 - 2p \cos \pi x + p^2) \qquad 0 < x < 2 \qquad p^2 \leq 1$$

Taking then the pressure at the well ($x = x_w + r_w$; $y = y_w + r_w$), and substituting into Eq.4 in the text, finally yields an exact analytical expression for the shape factor :

$$\ln C_A = 0.8091 + \ln 4\pi^2 + \ln \frac{x_e}{y_e} - \frac{\pi}{3}\frac{x_e}{y_e}\left[1 - 3\frac{x_w}{x_e} + 3\left(\frac{x_w}{x_e}\right)^2\right] + \pi\sqrt{\frac{x_e}{y_e}}\left(1 - \frac{x_w}{x_e}\right)\frac{r_w}{\sqrt{A}} - 2\pi\frac{r_w^2}{A}$$

$$+ 1/4 \ln \left\{\left[1 + \frac{2\cos\frac{\pi}{2}\left(2\frac{r_w}{\sqrt{A}}\sqrt{\frac{x_e}{y_e}} + \frac{y_w}{y_e}\right)\sin\frac{\pi}{2}\frac{y_w}{y_e}}{\sin \pi\frac{r_w}{\sqrt{A}}\sqrt{\frac{x_e}{y_e}}}\right]\left[1 + \frac{\left[\cos 2\pi\frac{r_w}{\sqrt{A}}\sqrt{\frac{x_e}{y_e}} - e^{-2\pi\frac{x_e}{y_e}\frac{x_w}{x_e}}\right]^2}{\sin^2 2\pi\frac{r_w}{\sqrt{A}}\sqrt{\frac{x_e}{y_e}}}\right]\left[1 + \frac{\left[\cos 2\pi\left(\frac{r_w}{\sqrt{A}}\sqrt{\frac{x_e}{y_e}} + \frac{y_w}{y_e}\right) - e^{-2\pi\frac{x_e}{y_e}\frac{x_w}{x_e}}\right]^2}{\sin^2 2\pi\frac{r_w}{\sqrt{A}}\sqrt{\frac{x_e}{y_e}}}\right]\right\}$$

$$- \sum_{n=1}^{\infty}\frac{1}{n} e^{-2n\pi\frac{x_e}{y_e}\left(1 - \frac{x_w}{x_e}\right)} \frac{\left[1 + e^{-2n\pi\frac{x_e}{y_e}\frac{x_w}{x_e}}\right]^2}{1 - e^{-2n\pi\frac{x_e}{y_e}}} \cos n\pi\frac{y_w}{y_e} \cos n\pi\left(\frac{y_w}{y_e} + 2\frac{r_w}{\sqrt{A}}\sqrt{\frac{x_e}{y_e}}\right) \qquad \text{(A-2)}$$

with $\frac{r_w}{\sqrt{A}}\sqrt{\frac{y_e}{x_e}} + \frac{x_w}{x_e} < 1$; $\frac{r_w}{\sqrt{A}}\sqrt{\frac{y_e}{x_e}} < 1$; and $\frac{r_w}{\sqrt{A}}$ small compared to 1.

APPENDIX B

SHAPE FACTOR FOR A FRACTURED WELL IN A CLOSED RECTANGLE

An expression for the dimensionless pressure function for a vertically fractured well in a rectangle has been presented by Gringarten, et al. in Ref. 12. With the well reservoir system sketched in Fig.3, Eq.27 of Ref.12 becomes :

$$P_D(t_{DA}) = 2\pi\int_0^{t_{DA}}\left[1 + 2\sum_{n=1}^{\infty}\exp\left(-n^2\pi^2\frac{x_e}{y_e}\tau\right)\cos\frac{n\pi}{2}\left(1 + \frac{y_w}{y_e}\right)\cos\frac{n\pi}{2}\left(1 + \frac{y_w}{y_e} + 2\frac{y}{x_f}\frac{x_f}{\sqrt{A}}\sqrt{\frac{x_e}{y_e}}\right)\right]$$

$$\left[1 + 2\sum_{n=1}^{\infty}\exp\left(-n^2\pi^2\tau\Big/\frac{x_e}{y_e}\right)\frac{\sin n\pi\frac{x_f}{\sqrt{A}}\Big/\sqrt{\frac{x_e}{y_e}}}{n\pi\frac{x_f}{\sqrt{A}}\Big/\sqrt{\frac{x_e}{y_e}}}\cos\frac{n\pi}{2}\left(1 + \frac{x_w}{x_e}\right)\cos\frac{n\pi}{2}\left(1 + \frac{x_w}{x_e} + 2\frac{x}{x_f}\frac{x_f}{\sqrt{A}}\Big/\sqrt{\frac{x_e}{y_e}}\right)\right]d\tau \qquad \text{(B-1)}$$

Performing the integration, taking the limit at long times and using the various summation formulas presented in Appendix A, yields a closed analytical expression for the pseudo-steady state form of Eq.B-1 . The result is written as Eq.13 in the text, with

$$
\begin{aligned}
(p_{int})_{Df} = {} & \frac{\pi}{6}\,\frac{x_e}{y_e} + \pi\left(\frac{x}{x_f}\right)^2\left(\frac{x_f}{\sqrt{A}}\right)^2 + \pi\,\frac{x}{x_f}\,\frac{x_f}{\sqrt{A}}\,\frac{x_w}{x_e}\sqrt{\frac{x_e}{y_e}} + \frac{\pi}{2}\,\frac{x_e}{y_e}\left(\frac{x_w}{x_e}\right)^2 - \frac{\pi}{2}\,\frac{x_f}{\sqrt{A}}\sqrt{\frac{x_e}{y_e}} + \frac{\pi}{3}\left(\frac{x_f}{\sqrt{A}}\right)^2 \\
& - \frac{\pi}{2}\left(\frac{x}{x_f}\right)^2\frac{x_f}{\sqrt{A}}\sqrt{\frac{x_e}{y_e}} - \frac{\pi}{2}\left(\frac{x}{x_f}\right)\frac{x_w}{x_e}\,\frac{x_e}{y_e} - \frac{\pi}{4}\,\frac{\sqrt{A}}{x_f}\left(\frac{x_e}{y_e}\right)^{\frac{3}{2}}\left(\frac{x_w}{x_e}\right)^2 + \frac{\pi}{12}\,\frac{\sqrt{A}}{x_f}\sqrt{\frac{y_e}{x_e}} \\
& + \frac{\pi}{2}\left(\frac{y}{x_f}\right)^2\frac{x_f}{\sqrt{A}}\sqrt{\frac{x_e}{y_e}} - \frac{\pi}{2}\left(\frac{y}{x_f}\right) + \frac{\pi}{2}\left(\frac{y}{x_f}\right)\left(\frac{y_w}{y_e}\right) - \frac{\pi}{4}\,\frac{\sqrt{A}}{x_f}\sqrt{\frac{y_e}{x_e}}\,\frac{y_w}{y_e} + \frac{\pi}{4}\,\frac{\sqrt{A}}{x_f}\sqrt{\frac{y_e}{x_e}}\left(\frac{y_w}{y_e}\right)^2 \\
& - \frac{1}{8\pi}\,\frac{\sqrt{A}}{x_f}\sqrt{\frac{y_e}{x_e}}\sum_{n=1}^{\infty}\frac{1}{n^2}\cos n\pi\,\frac{y_w}{y_e}\,\cos n\pi\left(\frac{y_w}{y_e} + \frac{y}{x_f}\,2\,\frac{x_f}{\sqrt{A}}\sqrt{\frac{y_e}{x_e}}\,\frac{x_e}{y_e}\right) \\
& e^{-n\pi\,\frac{x_e}{y_e}\left(2\,\frac{x_f}{\sqrt{A}}\sqrt{\frac{y_e}{x_e}} - \frac{x}{x_f}\,2\,\frac{x_f}{\sqrt{A}}\sqrt{\frac{y_e}{x_e}} - 2\,\frac{x_w}{x_e}\right)}\;\frac{1}{1 - e^{-2n\pi\frac{x_e}{y_e}}} \\
& \left[1 - e^{-2n\pi\,\frac{x_e}{y_e}\left(1 - 2\,\frac{x_f}{\sqrt{A}}\sqrt{\frac{y_e}{x_e}}\right)}\right]\left[1 + e^{-2n\pi\,\frac{x_e}{y_e}\left(\frac{x}{x_f}\,2\,\frac{x_f}{\sqrt{A}}\sqrt{\frac{y_e}{x_e}} + 2\,\frac{x_w}{x_e}\right)}\right] \\
& \left[1 + e^{-2n\pi\,\frac{x_e}{y_e}\,\frac{x_w}{x_e}}\;\frac{1 + e^{-2n\pi\,\frac{x_e}{y_e}\,\frac{x}{x_f}\,2\,\frac{x_f}{\sqrt{A}}\sqrt{\frac{y_e}{x_e}}}}{1 + e^{-2n\pi\,\frac{x_e}{y_e}\left(\frac{x}{x_f}\,2\,\frac{x_f}{\sqrt{A}}\sqrt{\frac{y_e}{x_e}} + 2\,\frac{x_w}{x_e}\right)}}\right]
\end{aligned}
\qquad (B\text{-}2)
$$

with $\frac{x_f}{\sqrt{A}}\sqrt{\frac{y_e}{x_e}}\left(1 - \frac{x}{x_f}\right) > \frac{x_w}{x_e}$; $\frac{x}{x_f} < 1$ and $\frac{x_f}{x_e} < 1$

The fractured well shape factor C_f is then obtained from $(p_{int})_{Df}$ as defined in Eq.14.

TABLE 1 : CORRESPONDANCE BETWEEN $\frac{x_f}{\sqrt{A}}$ AND $\frac{x_f}{x_e}$

x_e/y_e \ $x_f/\sqrt{A}$	0.5	0.3	0.2	0.15	0.10	0.05
1/4			1.25	1.67	2.50	5.00
1/2		1.18	1.77	2.36	3.54	7.07
1	1.00	1.67	2.50	3.33	5.00	10.00
2	1.41	2.36	3.54	4.71	7.07	14.14
4	2.00	3.33	5.00	6.67	10.00	20.00

TABLE 2 : DATA FOR EXAMPLE TEST

P_i	=	1,895	psi
B	=	1.25	RB/STB
μ	=	1.0	cp
ϕ	=	0.14	
c_t	=	17.7	psi^{-1}
q	=	800	STB/D

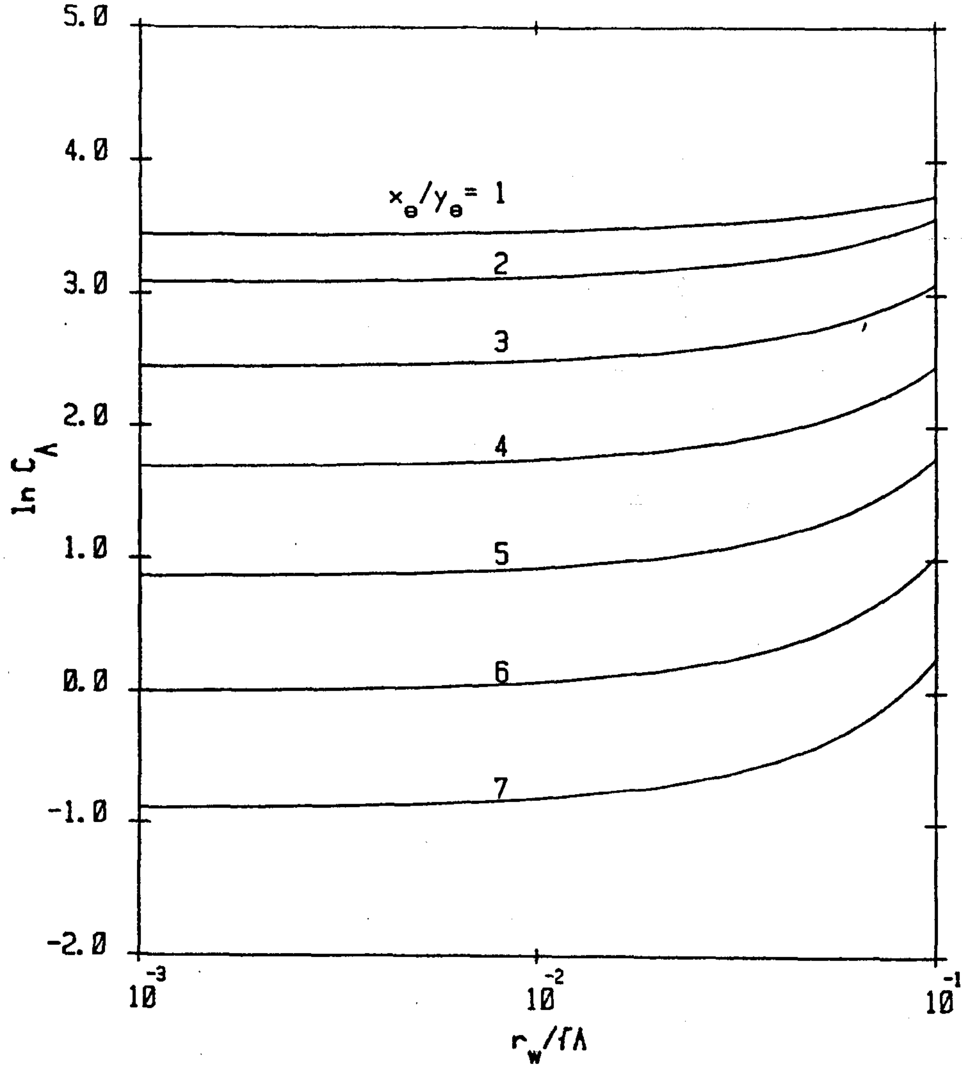

FIG.2: SHAPE FACTOR FOR AN UNFRACTURED WELL IN A CLOSED RECTANGLE

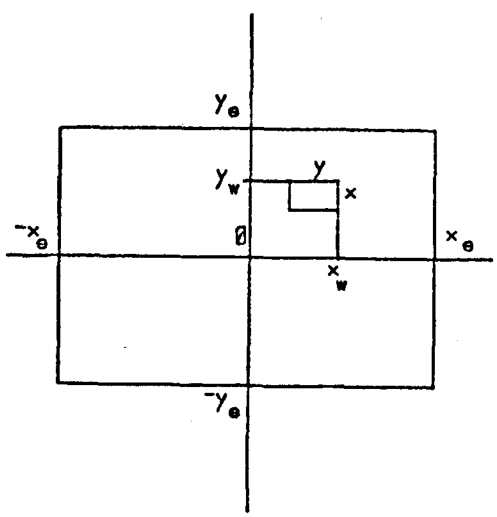

Fig. 1: Schematic of a well in a closed rectangle

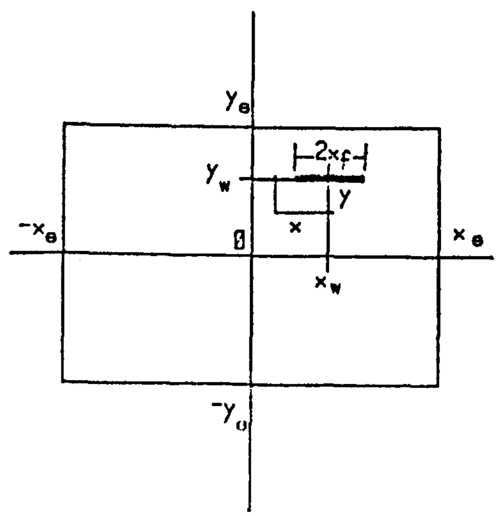

Fig. 3: Schematic of a fractured well in a closed rectangle

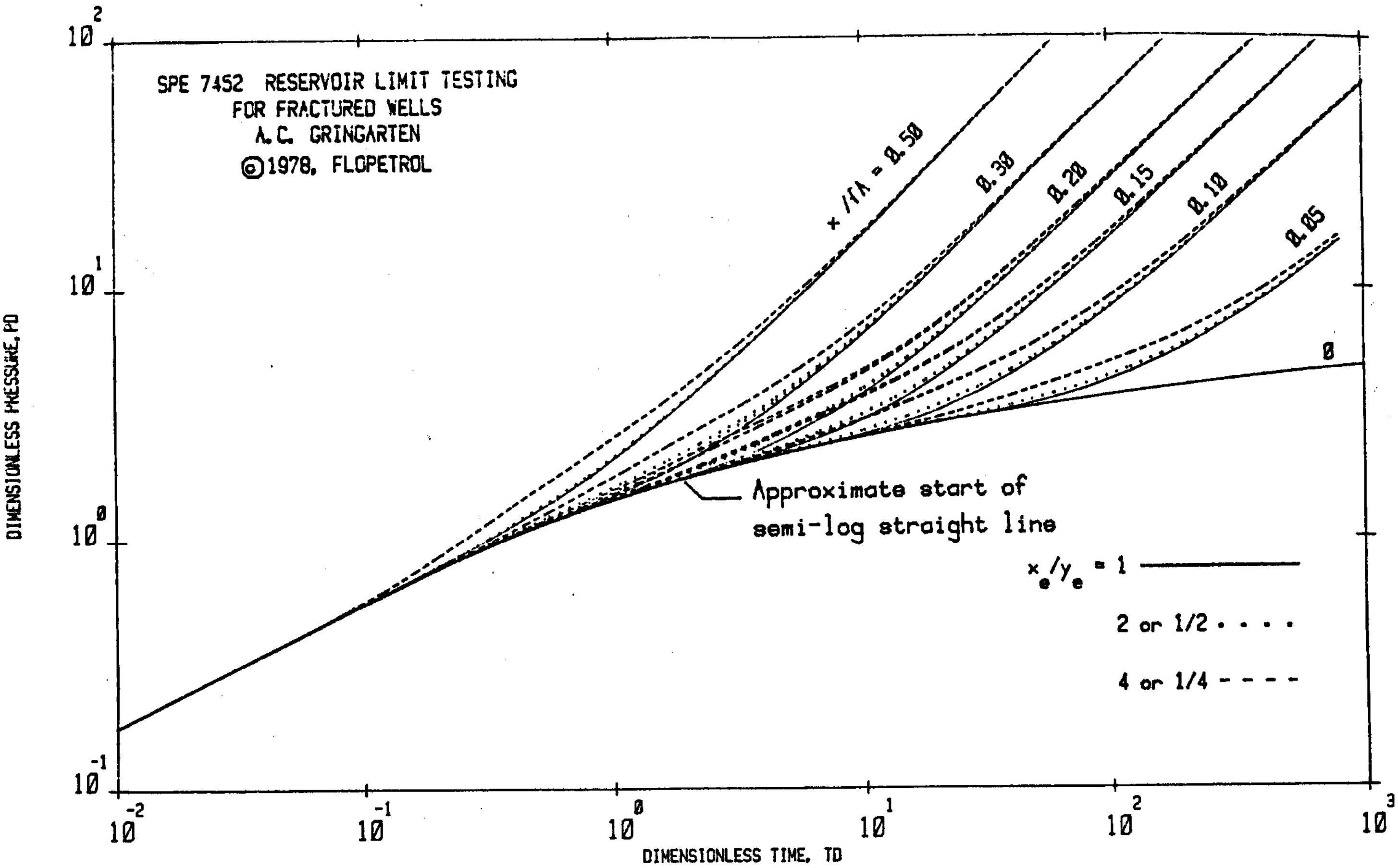

FIG.4 : WELL WITH A UNIFORM FLUX VERTICAL FRACTURE AT THE CENTER OF A CLOSED RECTANGLE

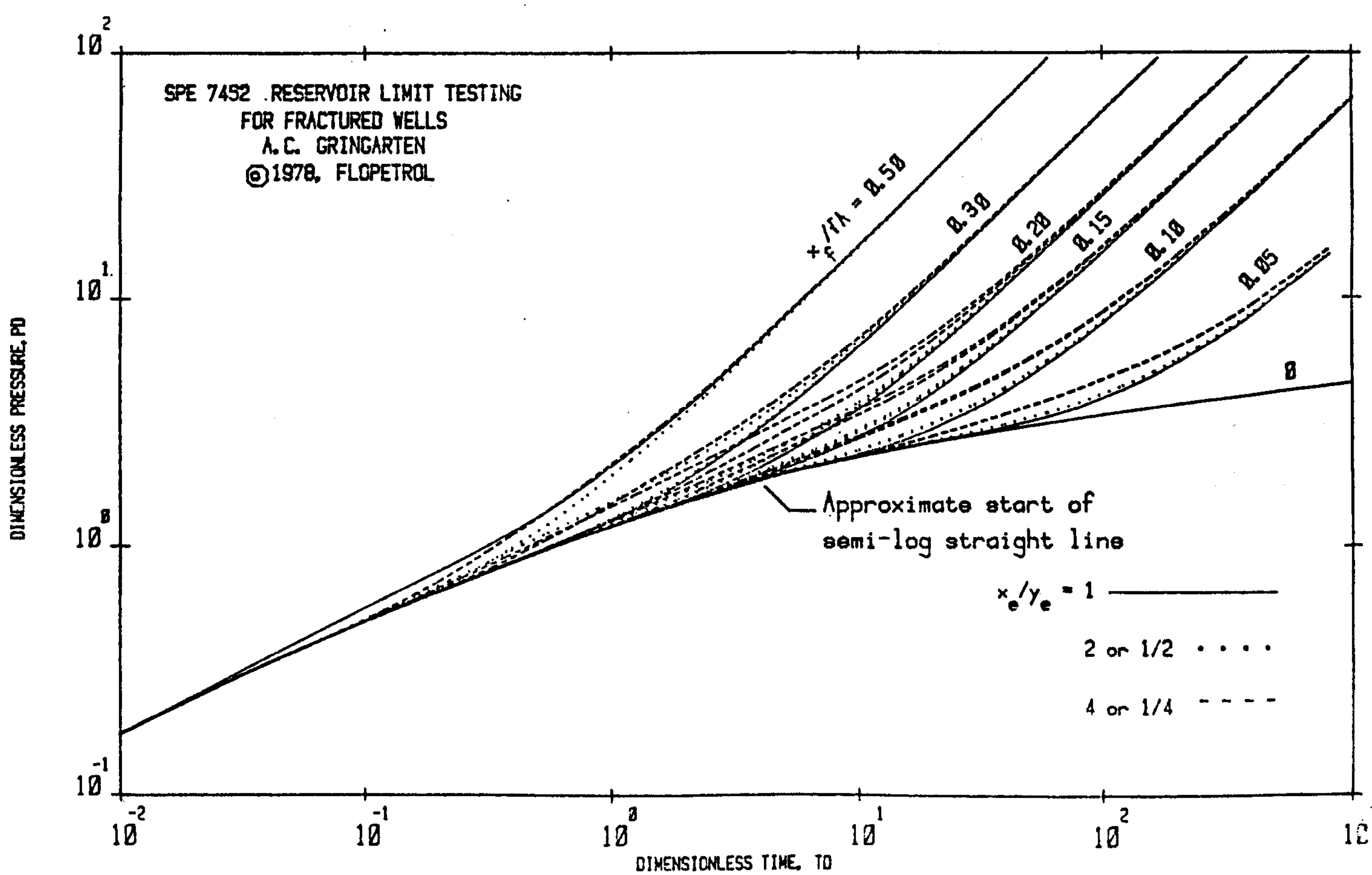

FIG.5 : WELL WITH AN INFINITE CONDUCTIVITY VERTICAL FRACTURE AT THE CENTER OF A CLOSED RECTANGLE

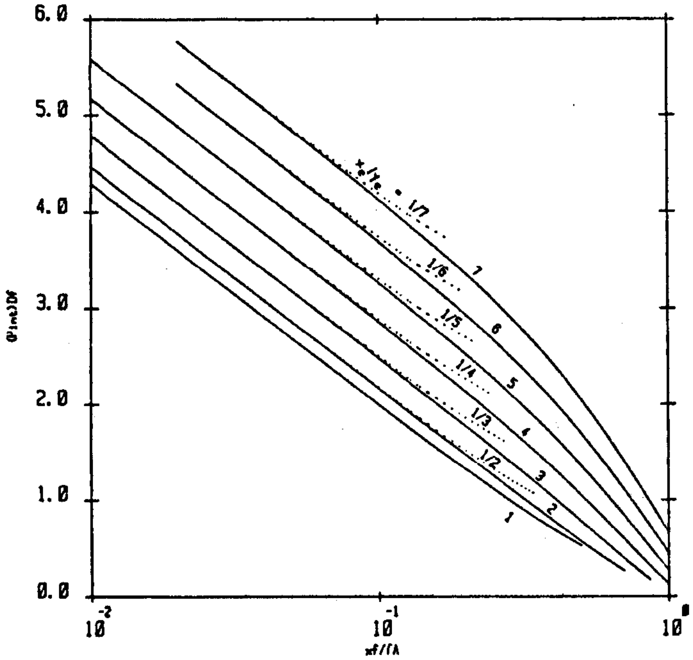

Fig.6 : (Pint)Df FOR A FRACTURED WELL IN A CLOSED RECTANGLE UNIFORM FLUX VERTICAL FRACTURE

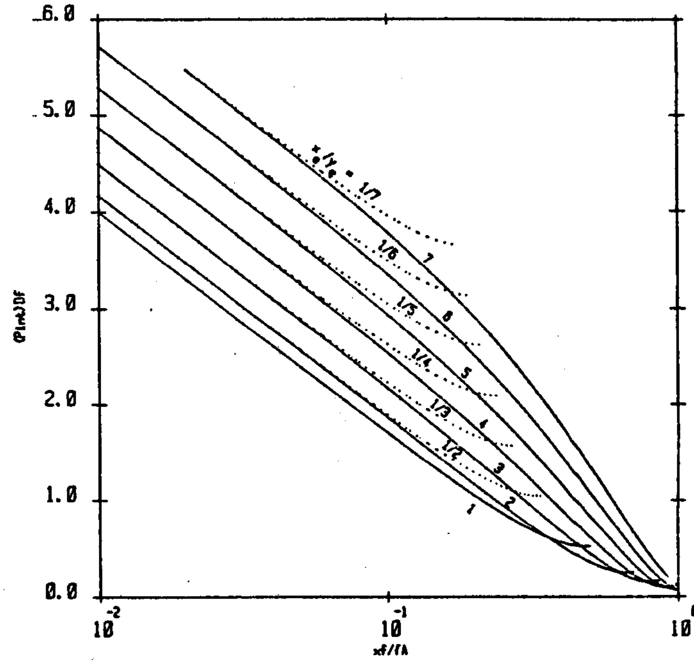

Fig.7: (Pint)Df FOR A FRACTURED WELL IN A CLOSED RECTANGLE INFINITE CONDUCTIVITY VERTICAL FRACTURE

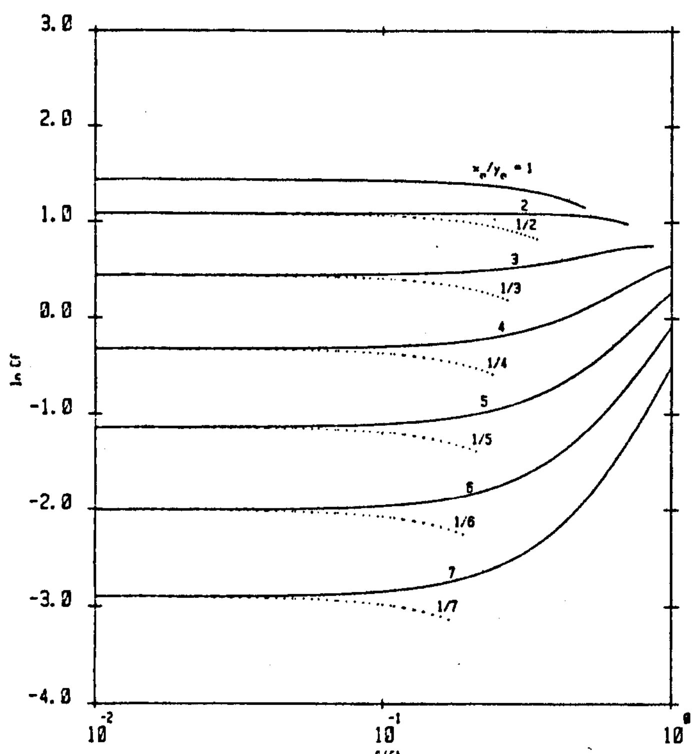

Fig.8: SHAPE FACTOR FOR A FRACTURED WELL IN A CLOSED RECTANGLE UNIFORM FLUX VERTICAL FRACTURE

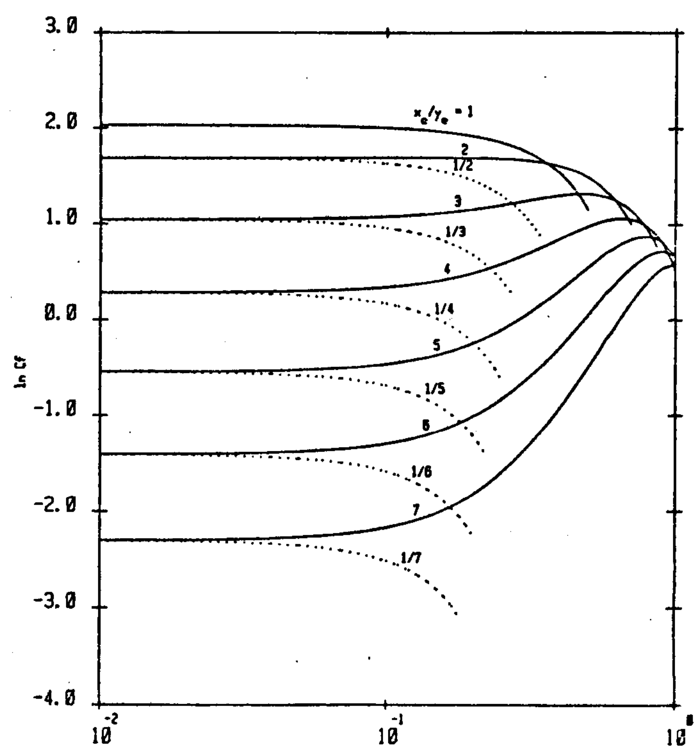

Fig.9: SHAPE FACTOR FOR A FRACTURED WELL IN A CLOSED RECTANGLE INFINITE CONDUCTIVITY VERTICAL FRACTURE

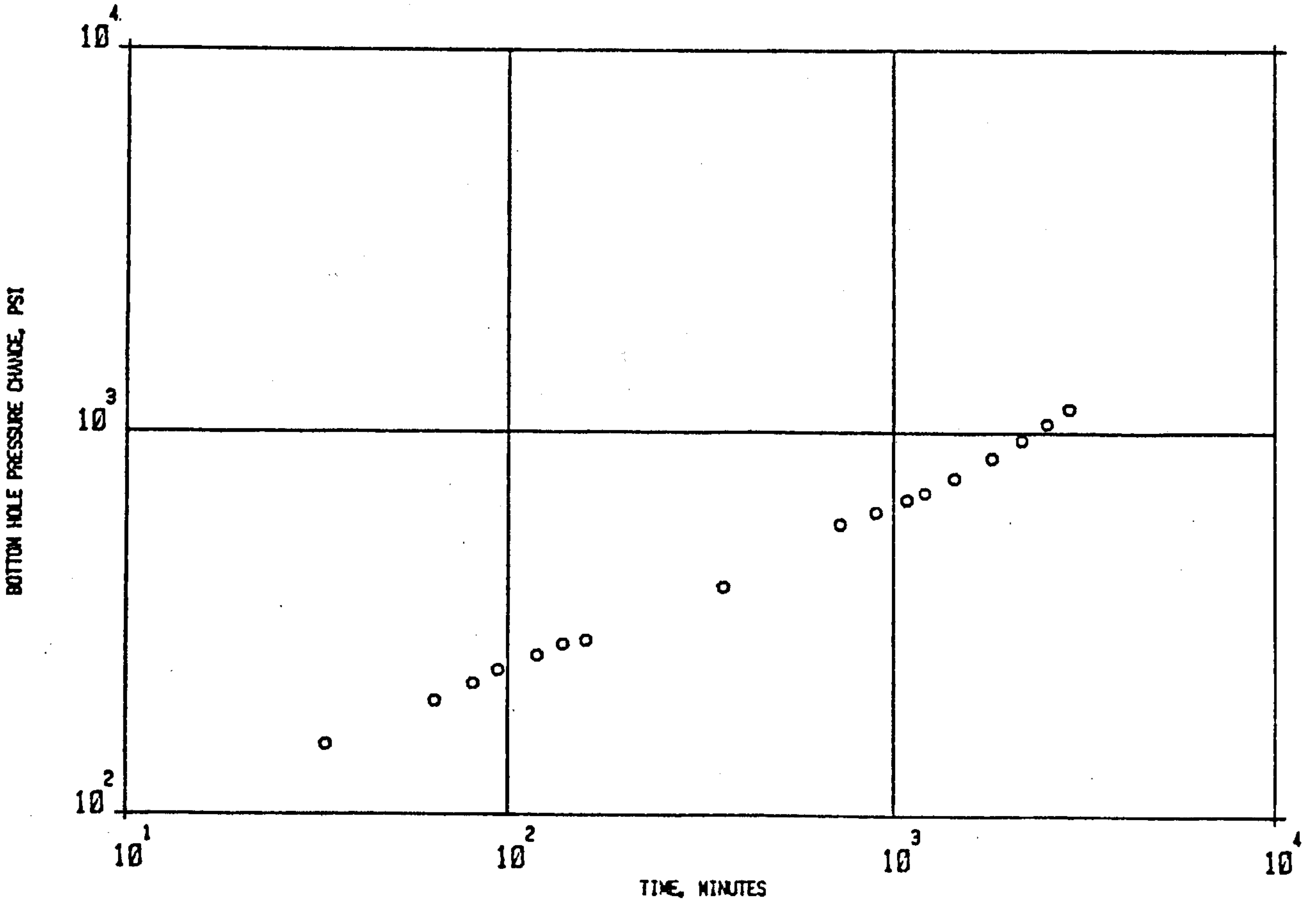

FIG. 10 : EXTENDED PRESSURE DRAWDOWN TEST
DENVER BASIN MUDDY SANDSTONE WELL (from Ref. 4)

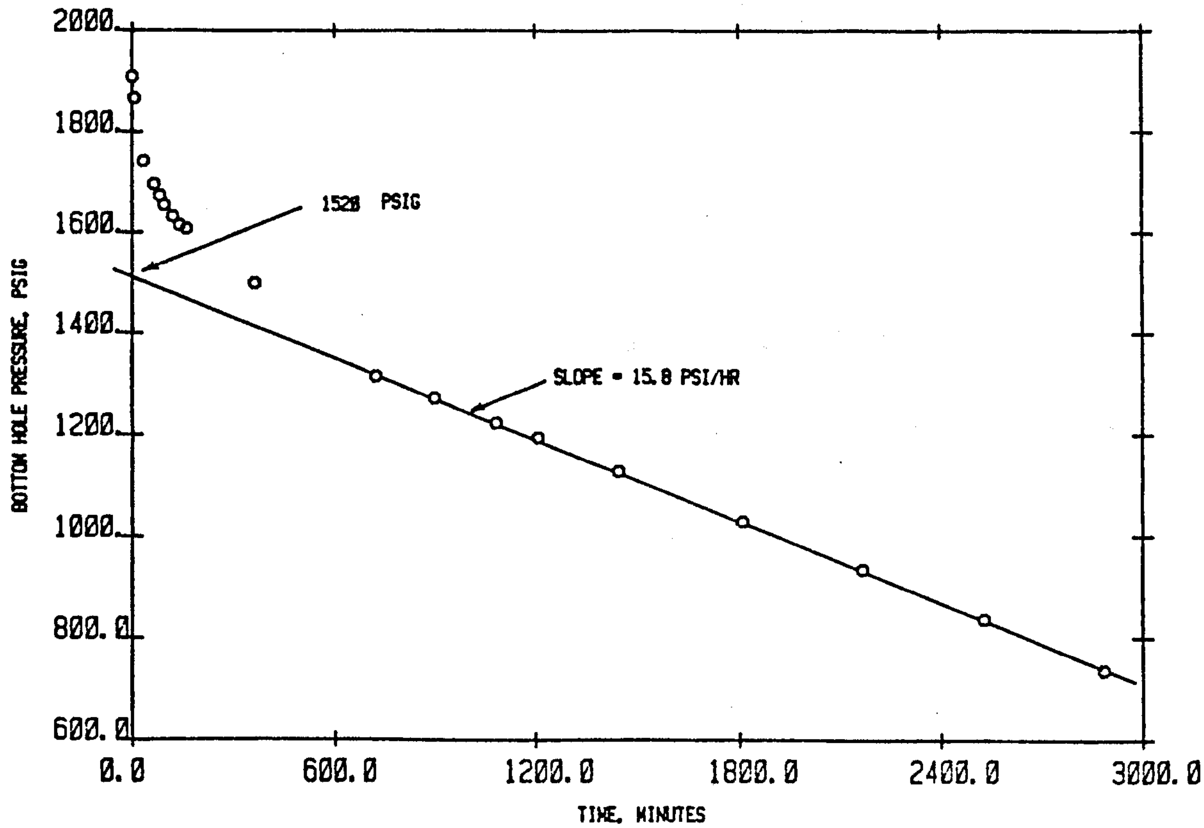

FIG. 11 : EXTENDED PRESSURE DRAWDOWN TEST
DENVER BASIN MUDDY SANDSTONE WELL

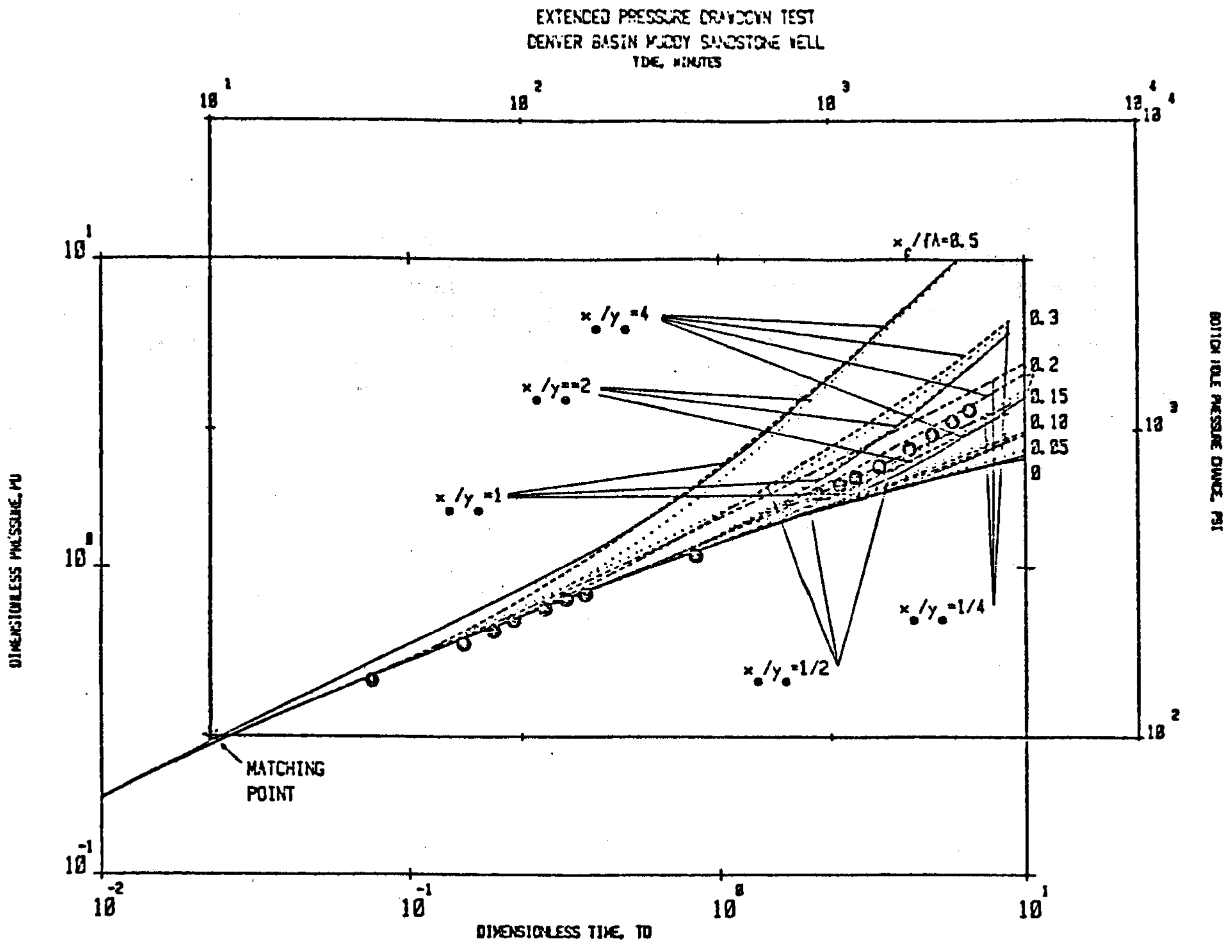

FIG. 12 : WELL WITH AN INFINITE CONDUCTIVITY VERTICAL FRACTURE AT THE CENTER OF A CLOSED RECTANGLE

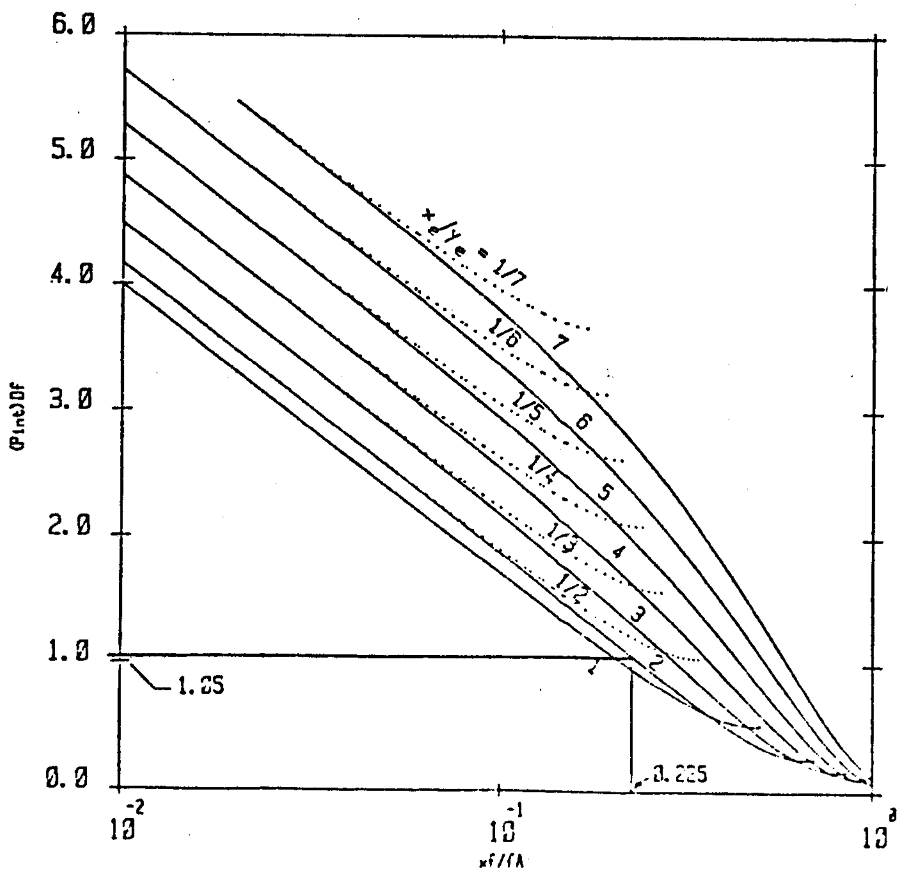

FIG. 13 : (Pint)DF FOR A FRACTURED WELL IN A CLOSED RECTANGLE